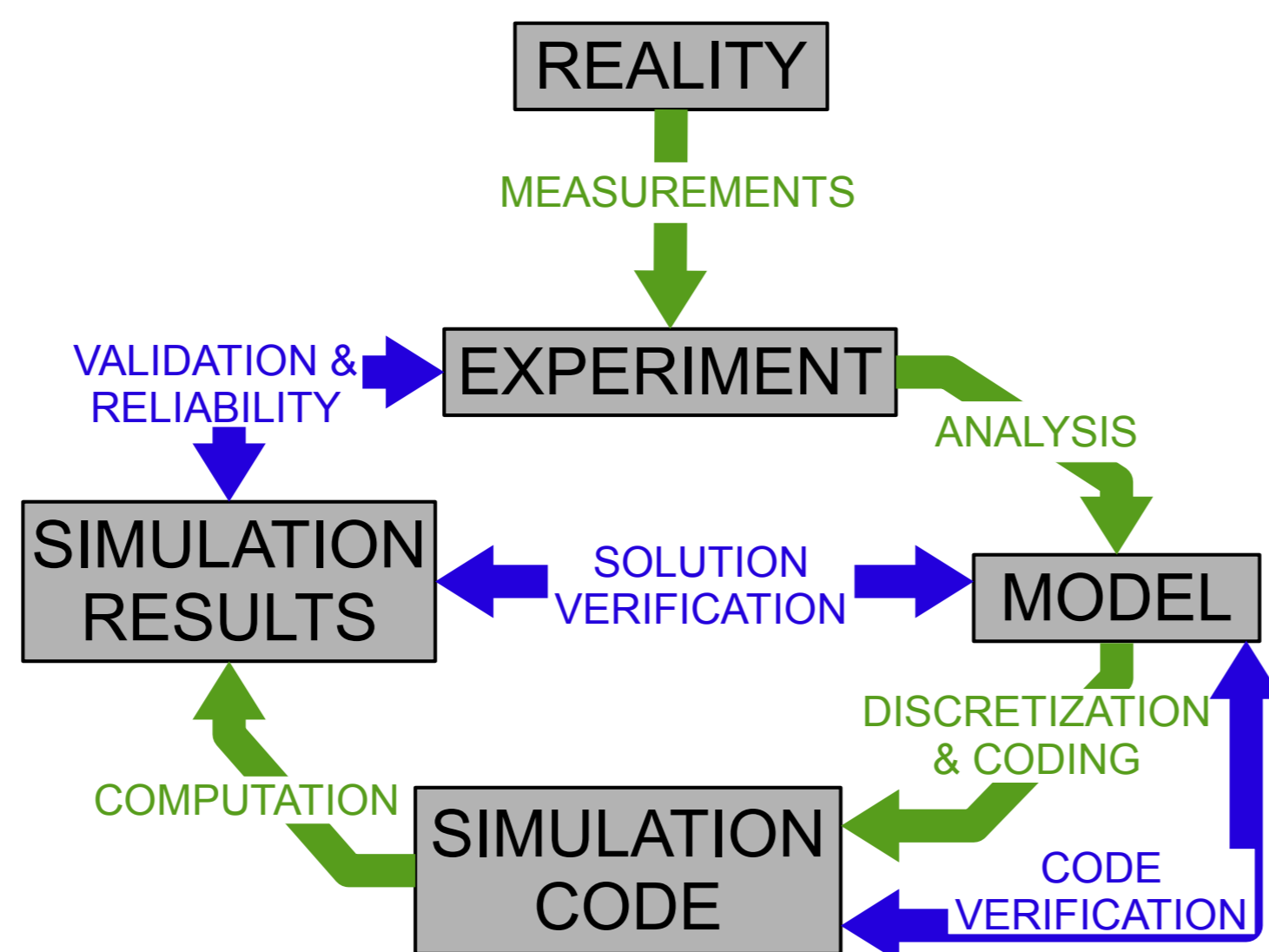


Introduction

The **Verification and Validation (V&V)** procedure assesses the reliability of numerical simulation codes by:

- Ensuring that the model equations are correctly implemented (**code verification**)
- Estimating the numerical error affecting simulations (**solution verification**)
- Assessing the consistency of the code results with experimentals (**validation**)

These procedures have been applied to GBS



Code verification methodology

Five different approaches have been developed for code verification procedure [Oberkampf et al.]:

- Simple tests
- Code-to-code comparisons (benchmarking)
- Discretization error quantification
- Convergence tests
- Order of accuracy tests**

The **order of accuracy tests** ensure both the correct coding of the model equations and the correct implementation of the chosen numerical scheme:

- Numerical error ϵ_h :

$$\epsilon_h = \|f_h - f\| = C_p h^p + O(h^{p+1})$$

where h represents the degree of refinement of the mesh, f_h the numerical solution and f the exact solution

- Observed order of accuracy \hat{p} :

$$\hat{p} = \frac{\ln(\epsilon_{rh}/\epsilon_h)}{\ln(r)}$$

- The code is verified if $\hat{p} \rightarrow p$ when the grid is refined (i.e., for $h \rightarrow 0$)

Method of manufactured solution (MMS): a systematic approach to perform order of accuracy test in absence of a known exact solution [Roache, Fluids Eng. 2001]:

- Choose an arbitrary analytical function g
- Compute the source term $S(g) = M(g)$ and subtract it from the numerical model
- Solve the modified model $M_h(g_h) - S = 0$
- Estimate the numerical error $\epsilon_h = \|g_h - g\|$
- Analyze the behavior of \hat{p} for $h \rightarrow 0$

The **manufactured solution** g should:

- Be general
- Be smooth enough and not singular
- Satisfy code constraints
- Avoid a term to overshadow the value of another

No physical constraints on the choice of g

Solution verification methodology

- An estimate of the exact solution f can be obtained by computing the **Richardson extrapolation** \bar{f} [Richardson, Philos. Trans. R. Soc. 1911]:

$$\bar{f} = f_h + \frac{f_h - f_{rh}}{r^p - 1} \quad \|\bar{f} - f\| = D_p h^{p+1} + O(h^{p+2})$$

- An approximation of the **discretization error** ϵ_h affecting the simulation results f_h is obtained:

$$\epsilon_h \simeq \|f_h - \bar{f}\| = \left\| \frac{f_{rh} - f_h}{r^p - 1} \right\|$$

Some constraints apply:

- Uniform mesh spacing
- Numerical solutions in the asymptotic regime
- No singularities or discontinuities

Moreover, it is required $\hat{p} \rightarrow p$ for $h \rightarrow 0$, where

$$\hat{p} = \frac{\ln[(f_{r^2h} - f_{rh}) / (f_{rh} - f_h)]}{\ln(r)}$$

- A more rigorous estimate of the relative discretization error is obtained by computing the **Grid Convergence Index (GCI)** [Roache, Fluids Eng. 1994]:

$$GCI = \frac{F_s}{r^{\hat{p}} - 1} \left| \frac{f_{rh} - f_h}{f_h} \right| \quad \begin{cases} F_s = 1.25 & \hat{p} = p \\ F_s = 3 & \hat{p} = \min[\max(0.5, \hat{p}), p] \\ F_s = 3 & \hat{p} = p \end{cases} \quad \begin{cases} \text{if } |(p - \hat{p})/p| \leq 10\% \\ \text{if } |(p - \hat{p})/p| > 10\% \\ \text{if } \hat{p} \text{ is unknown} \end{cases}$$

The Global Braginskii Solver (GBS) code

- Two-fluid Drift-reduced Braginskii equations**, $k_{\perp}^2 \gg k_{\parallel}^2$, $d/dt \ll \omega_{ci}$:

$$\frac{\partial n}{\partial t} = -\rho_*^{-1}[\phi, n] + \frac{2}{B}[C(p_e) - nC(\phi)] - \nabla_{\parallel}(n v_{\parallel e}) + S_n$$

$$\frac{\partial \omega}{\partial t} = -\rho_*^{-1}[\phi, \omega] - v_{\parallel i} \nabla_{\parallel} \omega + \frac{B^2}{n} \nabla_{\parallel} j_{\parallel} + \frac{2B}{n} C(p_e)$$

$$\frac{\partial v_{\parallel e}}{\partial t} = -\rho_*^{-1}[\phi, v_{\parallel e}] - v_{\parallel e} \nabla_{\parallel} v_{\parallel e} + \frac{m_i}{m_e} \left(\nu_{\parallel}^j + \nabla_{\parallel} \phi - \frac{1}{n} \nabla_{\parallel} p_e - 0.71 \nabla_{\parallel} T_e \right)$$

$$\frac{\partial v_{\parallel i}}{\partial t} = -\rho_*^{-1}[\phi, v_{\parallel i}] - v_{\parallel i} \nabla_{\parallel} v_{\parallel i} - \frac{1}{n} \nabla_{\parallel} p_e$$

$$\frac{\partial T_e}{\partial t} = -\rho_*^{-1}[\phi, T_e] - v_{\parallel e} \nabla_{\parallel} T_e + \frac{4 T_e}{3 B} \left[\frac{1}{n} C(p_e) + \frac{5}{2} C(T_e) - C(\phi) \right] + \frac{2}{3} T_e \left[0.71 \frac{\nabla_{\parallel} j_{\parallel}}{n} - \nabla_{\parallel} v_{\parallel e} \right] + S_{T_e}$$

- These equations are implemented in **GBS**, a **3D, flux-driven, global** turbulence code with circular geometry, and the system is closed by the Poisson's equation $\omega = \nabla_{\perp}^2 \phi$ [Ricci et al., PPCF 2012]
- System is completed with a set of **first-principles boundary conditions** applicable at the magnetic pre-sheath entrance where the magnetic field lines intersect the limiter [Loizu et al., PoP 2012]:

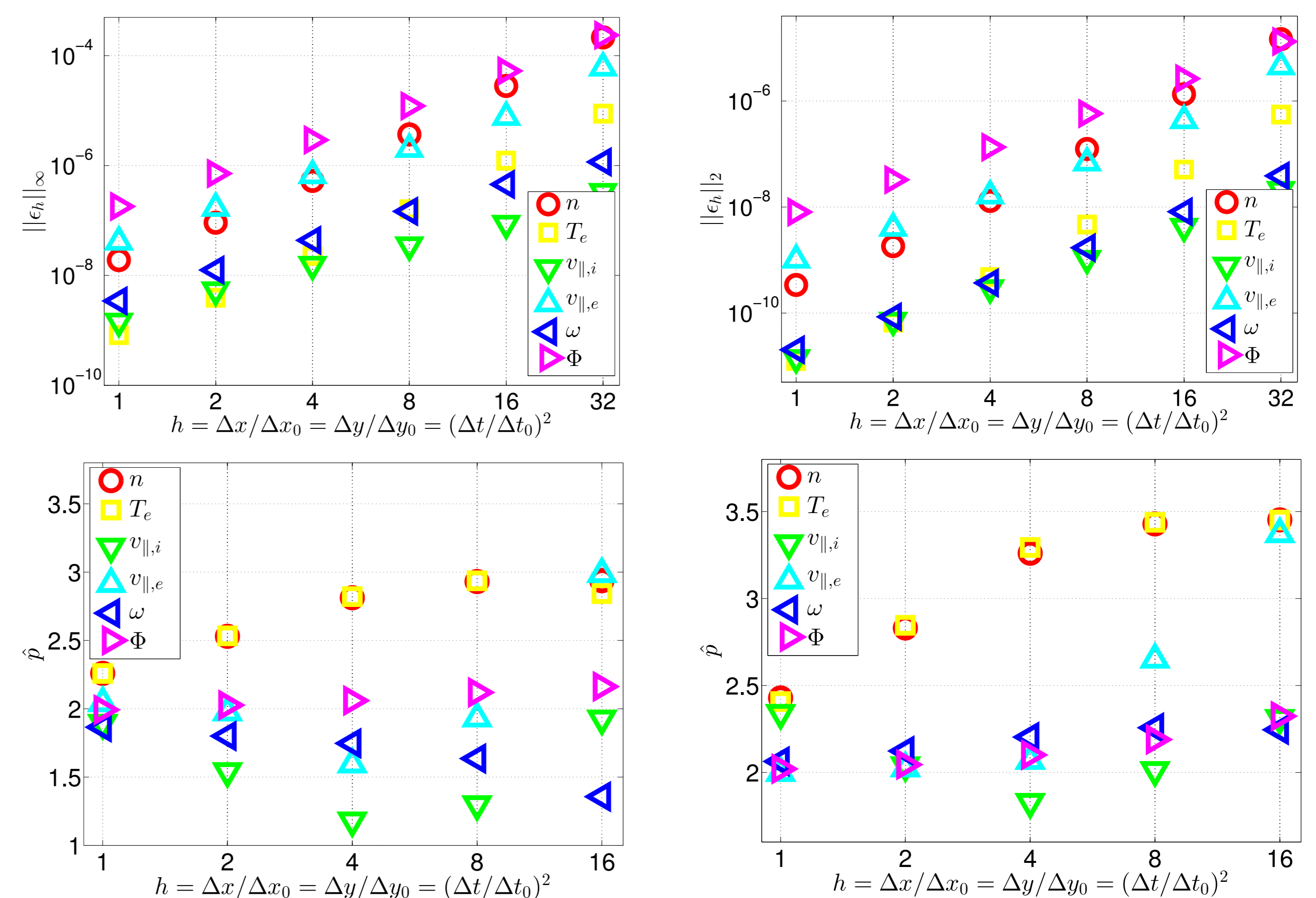
$$\begin{aligned} v_{\parallel i} &= \pm c_s & v_{\parallel e} &= \pm c_s \exp(\Lambda - \phi/T_e) \\ \partial_y T_e &= \kappa_T \partial_y \phi & \partial_y n &= \mp \frac{n}{c_s} \partial_y v_{\parallel i} \\ \omega &= -\cos^2 \alpha \left[(\partial_y v_{\parallel i})^2 \pm c_s \partial_y^2 v_{\parallel i} \right] & \partial_y \phi &= \mp c_s \partial_y v_{\parallel i} \end{aligned}$$

- Equations are discretized using a second second-order finite difference scheme in the spatial dimensions and the Arakawa scheme for Poissons brackets, time is advanced using a standard fourth-order Runge-Kutta scheme

- Note: normalized units used: $L_{\perp} \rightarrow \rho_s$, $L_{\parallel} \rightarrow R$, $t \rightarrow R/c_s$, $\nu = ne^2 R / (m_i \sigma_{\parallel} c_s)$

GBS verification results

- The **correct implementation** of the discretized equations is **verified** using MMS [Riva et al., PoP 2014]:



- The **estimate of the numerical error** affecting GBS results for standard mesh size (288, 120, 36) shows [Riva et al., PoP 2014]:

- Negligible numerical error for the pressure scale length
- Relative error for absolute value of n and T_e of the order of 20% – 25%

Development and achievements of GBS

The figure is a collage of images and diagrams. It includes:

- A diagram of a tokamak cross-section with labels for 'Limited SOL' and 'ITER-like SOL'.
- Photographs of tokamak experiments: LAPD, UCLA; Helimac, UTexas; HelCat, UNM; TORPEX, CRPP.
- Simulation results showing plasma profiles and turbulence structures.

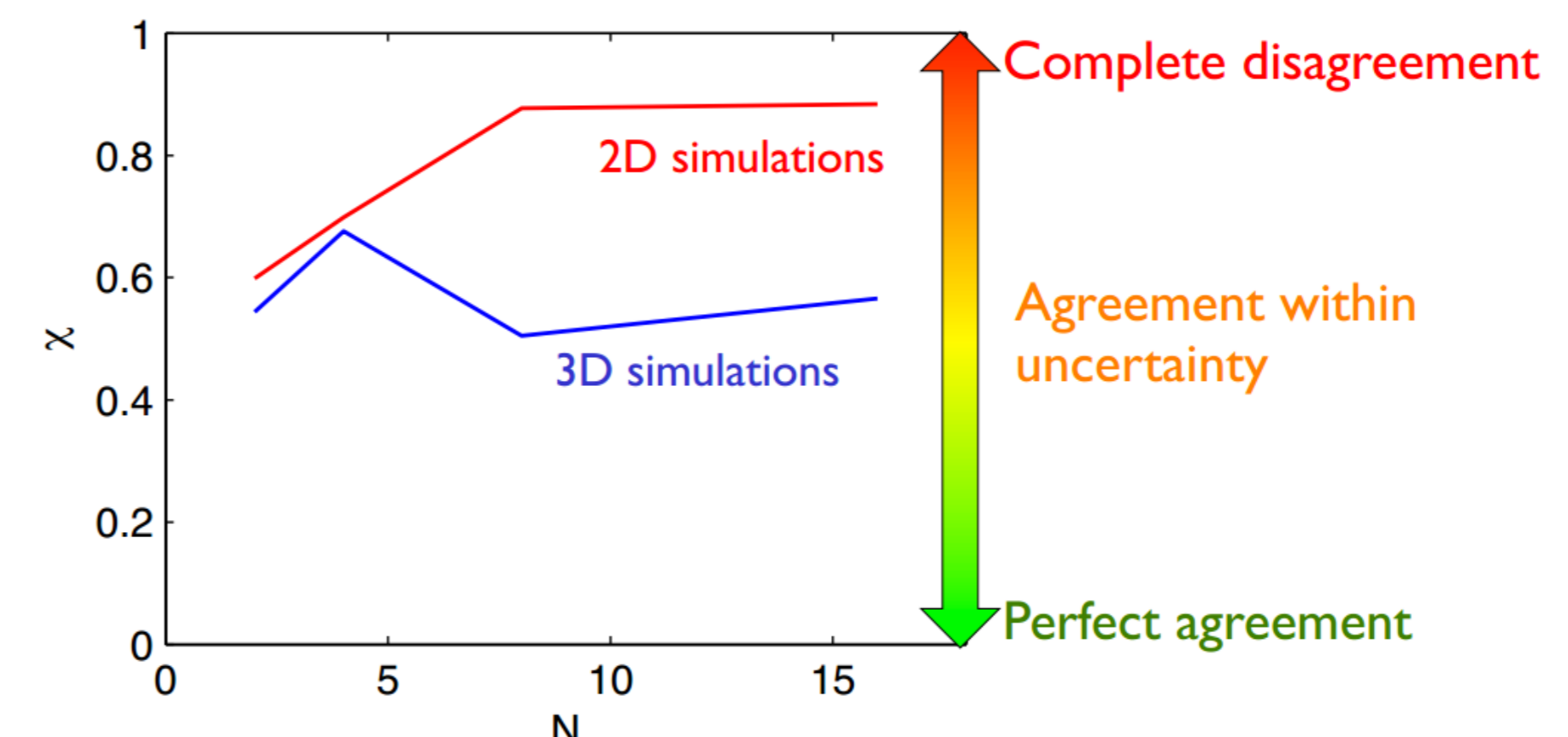
- Understanding turbulent regimes in TORPEX and LAPD
- SOL width scaling as a function of dimensionless / engineering plasma parameters
- Origin and nature of intrinsic toroidal plasma rotation in the SOL
- Non-linear turbulent regimes in the SOL
- Mechanism regulating the equilibrium electrostatic potential in the SOL

GBS validation results

- The **validation** procedure requires [Terry et al., PoP 2008; Greenwald, PoP 2010]:

- Identifying quantities we use for validation
- Estimating the uncertainties affecting measured and simulation data
- Evaluating the level of agreement for one observable, within its uncertainties
- Assessing how directly an observable can be extracted from simulation and experimental data
- Evaluating the global agreement

- GBS 2D and 3D model have been **validated against TORPEX experimental data** [Ricci et al., PoP 2011]:



- low N
- $k_{\parallel} = 0$
- Ideal interchange turbulence
- 2D model appropriated
- High N
- $k_{\parallel} \neq 0$
- Resistive interchange turbulence
- 2D model not appropriated

- The validation procedure enable us to:

- Compare different models
- Reveal physical phenomena
- Assess the predictive capability of a code

Conclusion

- Introduced in the plasma physics community a rigorous methodology for code and solution verification
- Verified the correct implementation of the model equations in GBS
- Estimated the numerical error affecting GBS results
- Validated the GBS results against TORPEX experimental data